



Zinc Oxide Nanoparticles Catalysed One-Pot Three-Component Reaction: A Facile Synthesis of 4-Aryl-NH-1,2,3-Triazoles

Parmita Phukan¹ · Soniya Agarwal¹ · Kalyanjyoti Deori¹ · Diganta Sarma¹

Received: 17 December 2019 / Accepted: 7 February 2020
© Springer Science+Business Media, LLC, part of Springer Nature 2020

Abstract

A facile one-pot, three component reaction has been developed using aldehydes, nitroalkane and sodium azide with zinc oxide nanocatalyst for the synthesis of 4-aryl-NH-1,2,3-triazoles. ZnO nanoparticles with controlled size (15–25 nm) and morphology were prepared using a sonochemical strategy. Structural and morphological study revealed the growth of well crystalline particles along the *c* axis i.e. [0001] direction due to higher surface energy. The catalysis protocol used in this work offers an efficient and highly economical alternative to the existing methods since the reactions proceed smoothly in green solvent polyethyleneglycol (PEG) 400 under aerobic condition. The reaction has a broad substrate scope resulting in excellent yields of the desired products. The catalyst recovery part was tricky at the initial stages; however an alternative route was successfully introduced to recover the former and reused it for the next cycles of catalytic reaction with excellent retentivity in the catalytic activity. The observed high catalytic efficacy with no significant activity loss using recovered catalyst is mainly due to the retention of morphology and crystal structure of ZnO nanoparticles after many catalytic reactions.

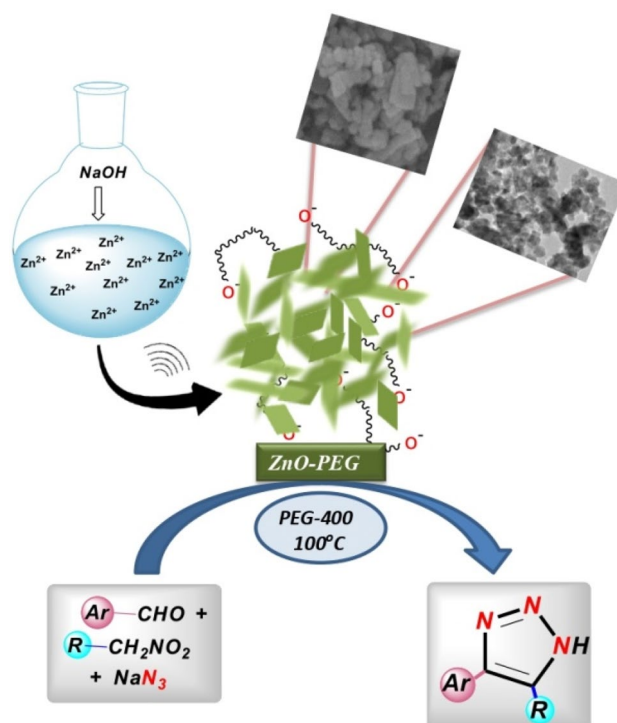
Electronic supplementary material The online version of this article (<https://doi.org/10.1007/s10562-020-03143-w>) contains supplementary material, which is available to authorized users.

✉ Kalyanjyoti Deori
kalchemdu@gmail.com

✉ Diganta Sarma
dsarma22@gmail.com

¹ Department of Chemistry, Dibrugarh University, Dibrugarh, Assam 786004, India

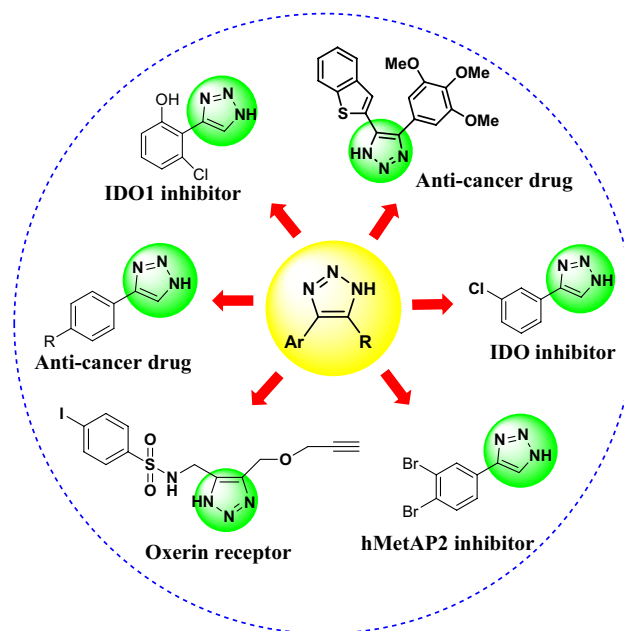
Graphic abstract



Keywords One-pot · Multicomponent reaction (MCR) · Green chemistry · Zinc oxide nanoparticles · Poly (ethylene glycol) (PEG) · 4-Aryl-NH-1,2,3-triazoles

1 Introduction

Over the past few decades, much attention has been paid on the development of novel methodologies to prepare active pharmacological agents that serve as new approaches to drug discovery. Multi-component reactions (MCRs) are of significant importance for such discoveries over conventional linear type syntheses [1]. In such reactions, three or more reactants are taken in one pot to form a novel product which contains portions of individual reactants. Multi-component reaction strategy offers remarkable advantages such as operational simplicity, reduction in number of work-up steps thus reducing waste, considerably short reaction time, efficiency and effectiveness in drug discovery research. Hence, design of new MCRs have acquired considerable interest as it may offer greater possibilities in synthetic processes by minimizing waste generation, time and effort. The first multicomponent reaction (MCR) was reported by Laurent and Gerhardt in 1838 [2]. Since then, many name reactions have been incorporated in MCRs such as Biginelli, Mannich, Grieco, Hantzsch, Tietze, Ugi, Robinson–Schopf etc. [3, 4] including the synthesis of 1,2,3-triazoles [5, 6]. Following historic studies in 2002 [7, 8], 1,2,3-triazole compounds



Scheme 1 Schematic diagram showing importance of NH triazole in various bioactive molecules

have established a tremendous and widespread impact on the field of chemical science. Owing to their wide chemical versatility, triazoles show considerable importance in diverse disciplines ranging from organic synthesis and material science to nanotechnology and drug discovery [9–11]. This class of compounds are of utmost importance in industrial applications such as photo-stabilizers, agrochemicals, dyes, materials and corrosion inhibitors [12–14]. Moreover, 1,2,3-triazoles possess a wide spectrum of medicinal properties such as herbicidal, anti-allergic, anti-bacterial and anti-HIV properties [15–18]. Especially, 4-aryl-1,2,3-triazoles possess interesting medicinal values to treat various types of serious diseases such as cancer, Alzheimer's disease, AIDS, etc. (Scheme 1) [19]. Researchers revealed that many drugs and natural products are composed of amide bonds. More than 25% of all drugs contain at least one amide bond. NH-triazoles possess some of the unique properties that make them remarkable mimetics of amide bonds [20–26]. Hence, this class of heterocyclic compounds has been effectively utilized in drug discovery [27, 28].

Moreover, there has been an increasing awareness in the need of sustainable strategies for the maintenance of “greenness” in various synthetic organic pathways [29, 30]. The entire academic and scientific community has been focusing on minimizing the use of volatile organic compounds (VOCs), hazardous reaction conditions and replace them by non-volatile, non-flammable and non-toxic greener alternative reaction medium. In this regard, the use of water, ionic liquids, supercritical fluids, glycerol, polyethylene glycol (PEG) etc. has become highly relevant in developing greener synthetic strategies [31–34]. The use of these environmentally friendly solvents can have significant advantages such as increased reaction rate, easy isolation of products etc. PEGs have emerged as a new beneficial class of green solvents because of their highly desirable properties such as non-toxic, non-volatile, chemically inert, commercially available and most importantly reusable [35–37]. All these factors encouraged us to switch our interest to use PEG as green reaction media and ZnO nanoparticles as non-toxic and highly stable catalyst.

ZnO is a commonly available metal oxide used since decades as an antibacterial, antioxidant [38], antiseptic [39], heterogeneous catalysts [40], in cancer cell treatment [41] and as semiconductor having wide band gap (3.37 eV) [42, 43]. Nano-ZnO counterparts are used as effective alternatives to many conventional catalysts [44] as they provide large surface area for reactivity, high stability under catalytic reaction condition and can be tuned to various morphologies like nanorods [45], nanowires [46], nanospheres [47], nanotetrapods [48, 49] by controlling various parameters such as reaction time, temperature, use of surface selective surfactants, surfactant to precursor ratio, reducing agent etc. [50]. Different synthetic processes also play a vital role

towards the development of its morphology. Here, in this work we have employed ultrasonication as a greener route for the preparation of ZnO nanoparticles as it diminishes the use of harsh temperature and additional eco-unfriendly additives to obtain homogeneously distributed and well crystalline nanoparticles. Ultrasonication is advantageous for nanoscale synthesis as it works on the principle of acoustic cavitations which involves the rise and fall of both temperature and pressure in short time width [51, 52]. For further control of the shape and size a non-ionic and low molecular weight polymer PEG-400, as capping agent was used. Furthermore, we have developed a multi-component reaction strategy, which provides a simple and rapid access to a broad library of NH-triazoles with varied substitution patterns. Our protocol is highly effective for the synthesis of NH-triazoles using polyethylene glycol capped zinc oxide nanoparticles with > 98% yield.

2 Experimental Section

2.1 Chemicals

Zinc acetate ($\text{Zn}(\text{OAc})_2 \cdot 2\text{H}_2\text{O}$, 98.5%, Finar), Polyethylene glycol-400 (PEG-400, Merck), absolute ethanol (Ethanol, 96%, Sigma Aldrich), Sodium Hydroxide (NaOH, 97%, Qualigens), Nitromethane (CH_3NO_2 , 98%, TCI), Nitroethane ($\text{C}_2\text{H}_5\text{NO}_2$, 98%, Spectrochem), Sodium Azide (NaN_3 , 99%, Spectrochem) and all aldehydes (Spectrochem with 98% purity) were purchased and used without any further purification. The products were purified by column chromatography (120–200 mesh) over silica gel. Thin-layer chromatography was carried out using silica gel 60F₂₅₄ plates and visualization was carried out with UV light.

2.2 Synthesis of ZnO Nanoparticles

A simple sonochemical technique was developed to synthesize purely crystalline ZnO nanoparticles with the help of $\text{Zn}(\text{OAc})_2 \cdot 2\text{H}_2\text{O}$ as zinc precursor and PEG-400 as capping agent. In a typical synthesis procedure $\text{Zn}(\text{OAc})_2 \cdot 2\text{H}_2\text{O}$ (1 mmol) was dissolved in 1:1 (20 mL) ethanol and deionised water, under stirring condition. On complete dissolution, 2 mL PEG-400 was added followed by drop wise addition of 0.4 N NaOH (5 mL) until complete precipitation. The resultant solution was then covered and placed in a sonicator under ultrasonic irradiation for 90 min. The as-obtained product formed due to acoustic cavitation was then centrifuged and washed with water and ethanol for three times to remove excess surfactants or any other soluble products. A part of the sample was air dried at 60 °C for 5 h and the other part was dispersed in acetone for further characterization.

2.3 General Procedure for the Synthesis of NH-1,2,3-Triazoles

The mixture of corresponding benzaldehyde (1 mmol), nitroalkane (2 mmol), NaN_3 (3 mmol), PEG capped ZnO nano catalyst (5 mg) were stirred at 100 °C in 3 mL PEG-400 solvent under air. The progress of the reaction was monitored by TLC. After completion of the reaction, the reaction mixture was cooled to room temperature and extracted with ethyl acetate (3×10 mL). The combined organic layer was dried over anhydrous Na_2SO_4 . The filtrate was concentrated under reduced pressure. The final product was purified by column chromatography over silica gel using hexane/ethyl acetate mixture. The products were characterized by NMR and mass spectroscopy.

2.4 Instrument Details

Powder X-ray diffraction (XRD) Measurements were performed with a Bruker D8 discover X-ray diffractometer employing monochromatized Cu K alpha radiation (1λ 1.54056 Å) at 298 K.

Transmission electron microscopy (TEM). Low resolution transmission electron microscopy (TEM) images, phase-contrast high-resolution TEM (HRTEM) images and selected area electron diffraction (SAED) measurements were performed with a Philips Technai G230 transmission electron microscope operating at an accelerating voltage of 200 kV.

Field emission scanning electron microscopy (FESEM). FESEM measurements were done on a FEI Quanta 200F equipped with Oxford-EDS system IE 250 X Max 80.

Thermogravimetric analysis (TG-DTA) The thermogravimetric analysis (TG-DTA) was performed in a Perkin Elmer STA 8000 instrument. The heating rate was 20 °C/min for the temperature range 0 °C to 1300 °C in a platinum pan.

Fourier transform infrared spectroscopy (FT-IR) A Perkin Elmer FT-IR 2000 spectrophotometer was used to record the FT-IR spectra ($4000\text{--}400\text{ cm}^{-1}$).

Nuclear magnetic resonance (NMR) ^1H and ^{13}C NMR spectra were recorded at 500 MHz and 125 MHz respectively, using a Bruker Ascend 500 MHz spectrophotometer.

3 Results and Discussion

3.1 Structural Purity and Morphology Study of ZnO Nanoparticles

The composition, phase purity and interference, if any, of the polymer on crystal planes of the synthesized ZnO-PEG were investigated by powder XRD. The XRD pattern of as synthesized ZnO nanoparticles in Fig. 1 shows peaks at

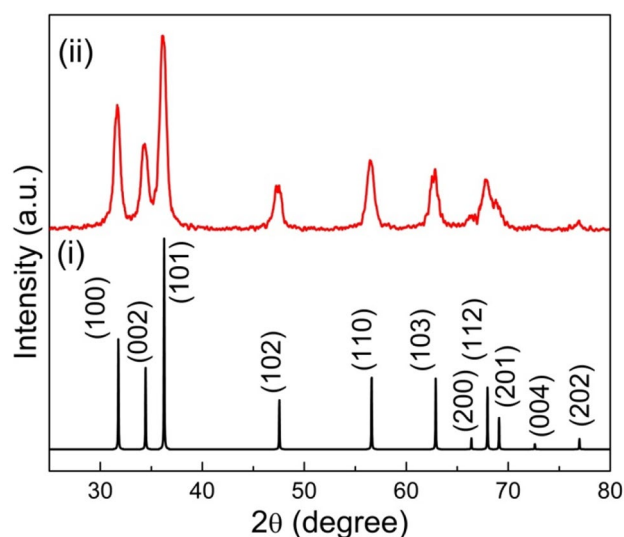


Fig. 1 Powder XRD pattern of (i) bulk ZnO and (ii) as-synthesized ZnO nanoparticles

$2\theta = 31.70, 34.37, 36.21, 47.41, 56.54, 62.89, 67.86, 69.02, 76.99$ corresponding to (100), (002), (101), (102), (110), (103), (200), (112), (201), (202) planes, respectively. These peaks are in complete agreement with the bulk XRD pattern of hexagonal wurtzite crystal structure of ZnO (space group: $P6_3mc$, $a = b = 3.2494$; $c = 5.2038$, JCPDS Card No. 005-0664) and no impurity peak for metallic zinc and $\text{Zn}(\text{OH})_2$ were observed. As there were no measurable shift observed in the peak positions between the experimental and bulk XRD patterns, this ruled out the possibility of any additional strain in the pure phase of as-synthesized ZnO nanoparticles. Both as-synthesized PEG-ZnO and the bulk ZnO do not have much difference in the peak intensity ratio as obtained from the XRD spectrum which leads to conclusion that there is no PEG interference on the crystal planes of ZnO but is actually adsorbed on the surface of the crystal. However, the distinct peak broadening in the experimental pattern (see Fig. 1) indicates the smaller grain boundaries of the as-synthesized particles. The crystallite size of PEG-ZnO was calculated to be 13 nm from the XRD pattern using Scherrer formula.

It is clearly seen from the low magnification TEM images shown in Fig. 2a that the as-prepared ZnO nanoparticles have small plate/sheet type of architecture whose sizes are in the range of 15–25 nm. When focused an individual nanoparticle under HRTEM it reveals clear lattice fringes of {002} facets of hexagonal wurtzite type structure with interplanar d -spacing of 0.53 nm (Fig. 2b). After nucleation the initial crystal growth along the c -axis i.e., [0001] direction of ZnO nanocrystals as shown in Fig. 2b (also see Fig. 2e for wurtzite type ZnO structure) are attributed to the high surface energy and polar nature of {0001} facets. The growth was further restricted probably due to the use of surfactant

Fig. 2 **a** Low magnification TEM image of the as-synthesized PEG capped ZnO nanoparticles. **b** HRTEM image of one ZnO particle showing (002) exposed planes along *c*-axis. **c** Corresponding 2D-FFT image calculated from the selected area of HRTEM image in (b). **d** Corresponding SAED pattern clearly showing predominant crystal planes of ZnO wurtzite structure. **e** A pictorial representation of hexagonal wurtzite structure. **f** Average particle size distribution histogram

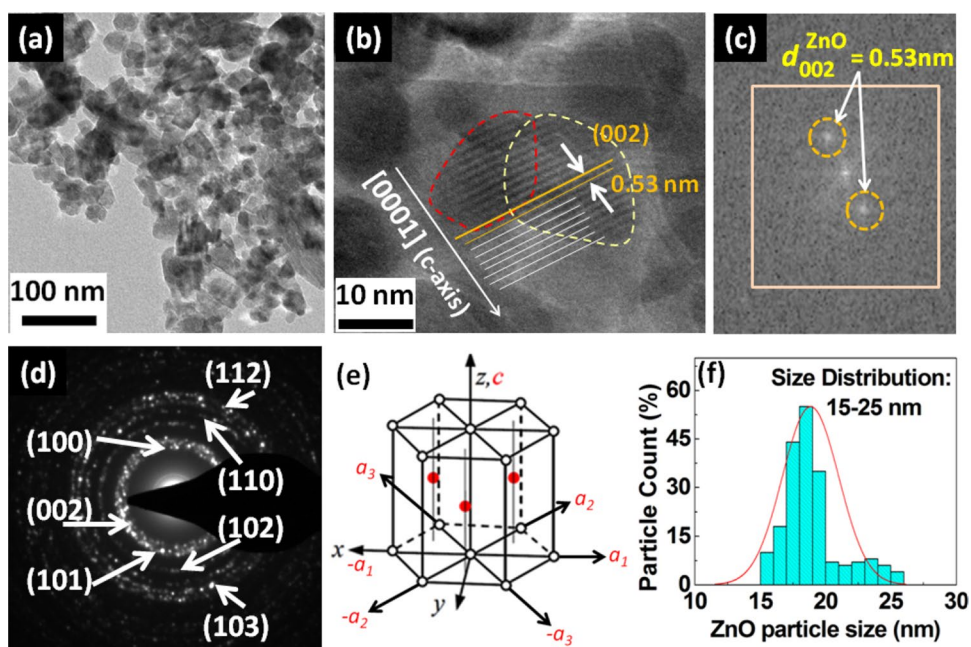
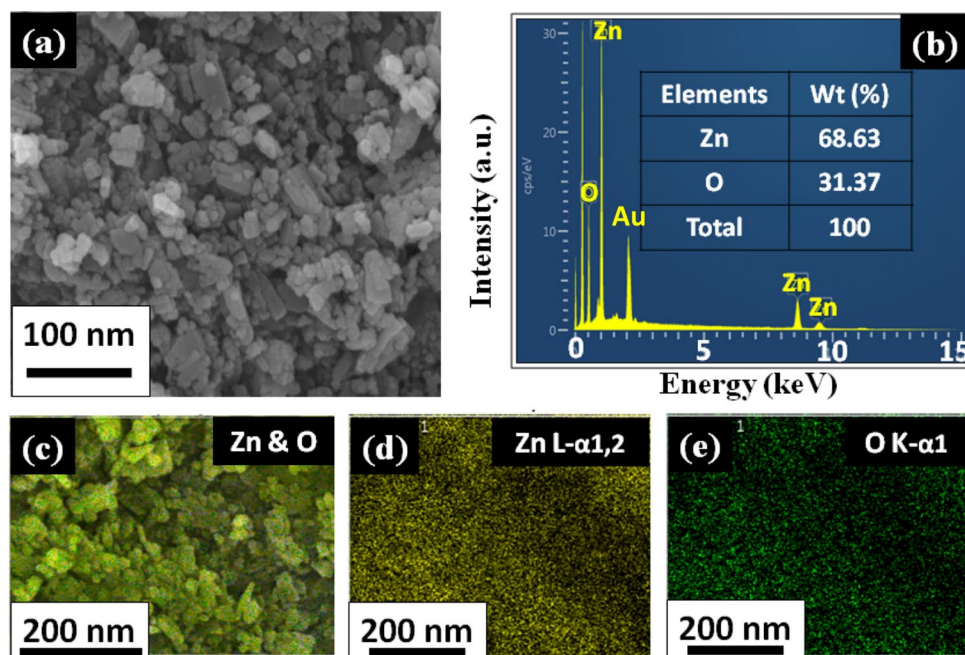


Fig. 3 **a** FESEM image of the as-synthesized PEG capped ZnO nanoparticles. **b** Representative SEM-EDS spectrum of the as-synthesized ZnO nanoparticles from different areas. SEM elemental mapping for stoichiometric characterization. **c** ZnO crystals showing both elements, **d** Zn and **e** O elemental maps showing distribution of both the elements in the sample from Zn L edge and O K edge respectively



PEG-400 and the final architecture thus obtained was kinetically favoured one. As evidenced from the FT-IR and thermal studies there were strong adsorption of PEG-400 on the surface of ZnO nanoparticles which do not exit up to 200 °C (see Figure S1). The peak at 543 cm^{-1} is the characteristic peak for Zn–O and the broad peak at 3416 cm^{-1} corresponds to hydroxyl group due to the PEG adsorption on ZnO. In addition to it the peaks at 2879 cm^{-1} (C–H stretching vibration), 1569 cm^{-1} , 1505 cm^{-1} and 1395 cm^{-1} (C–H bending vibration) revealed the presence of PEG.

Furthermore, the phase-contrast HRTEM image showing clear lattice fringes indicates the absence of any dislocations and stacking faults and the nature of particles are single crystalline. The two Dimensional Fast-Fourier Transform (2D-FFT) was generated from the selected section of as-synthesized ZnO crystal seen in panel 'b' and is shown in Fig. 2c, where exposure of highly energetic (002) planes can be unambiguously identified. The corresponding selected area electron diffraction (SAED) image as depicted in Fig. 2d showing spotty rings clearly revealed their pure

crystalline nature of as-synthesized ZnO nanoparticles. Various crystallographic planes viz., (100), (002), (101), (102), (110), (103), and (112) of hexagonal wurtzite structure were clearly indexed in this SAED pattern. Finally a narrow size distribution of 15–25 nm was obtained (as shown in Fig. 2f), from the size distribution histogram calculated for a large number of particles.

The surface topography along with the distribution of elements within the as-synthesized ZnO nanocrystals and the composition of the sample were investigated using high resolution field emission SEM (FESEM) and the results are shown in Fig. 3. FESEM image in Fig. 3a shows an unclear shape of ZnO nanoparticles with particle sizes ranging from 15 to 30 nm which is almost near to the particle size calculated from Scherrer formula (from corresponding XRD pattern) and consistent with HRTEM analysis. Elemental analysis via the Energy Dispersive X-ray Spectroscopy (EDS) under SEM-EDS mode revealed that there was no such compositional variation and the as-synthesized nanoparticles mainly consist of Zn and O with elemental ratio (Zn:O) of 1:1 (Fig. 3b). The appearance of gold (Au) peak in the spectra is due to gold coating of the sample during sample preparation. EDS technique was further applied via elemental mapping mode to confirm the uniform distribution of Zn and O among the hexagonal wurtzite structure of ZnO nanocrystals. Figure 3c showing both elements of ZnO crystals and Fig. 3d, e showing individual Zn and O element respectively are the clear evidences of homogeneous or symmetric distribution of constituent elements within the crystals.

Later on a potential mechanism of ZnO-PEG nanoparticle construction has been proposed in Scheme 2. $\text{Zn}(\text{OAc})_2 \cdot 2\text{H}_2\text{O}$ was ionised in ethanol and distilled water followed by precipitation with NaOH in presence of PEG-400. Drop wise addition of NaOH not only helps in the nucleation process but also restrict the growth of ZnO particles mainly along the [0001] direction as OH^- ions preferentially bind on {0001} surfaces. The polymer is adsorbed on the surface of the precipitate, which acts as a barrier and does not allow other particles to grow on it. The overall effect finally gives rise to very small sizes of (15–25 nm) irregular nanoplates/broken nanosheets type of architecture. Since PEG-400 is soluble in water and wide variety of

organic solvents, its presence makes the ZnO-PEG nanoparticles versatile in catalytic study.

3.2 Catalytic Study

We began to investigate the optimal parameters for the synthesis of NH-triazoles using 4-bromo-benzaldehyde, nitromethane and sodium azide as the model substrates under different reaction conditions. In our initial screening, we explored the most effective solvent and temperature condition for synthesis of NH-triazoles. A wide array of solvents including both organic and aqueous medium were examined (Table 1, entry 1–14). Interestingly, it was noticed that there is a significant variation in the yield of the desired products in each case. It can be seen from Table 1 that the best results were obtained when PEG-400 was used as solvent at 100 °C (Table 1, entry 10). The reaction was also carried out in water but very low yield of the product was observed (Table 1, entry 1). Subsequently, a range of solvents such as Dichloromethane (DCM), Dimethylformamide (DMF), Dimethylsulphoxide (DMSO), ethylene glycol and toluene were investigated but inferior yields of NH-triazoles were obtained (Table 1, entry 2–6). Further, in order to optimise the temperature, the cycloaddition reaction of 4-bromo-benzaldehyde, nitromethane and sodium azide was performed in PEG-400 solvent at 80 °C. Notably, the yield of the product went down at this temperature (Table 1, entry 11). Moreover, only a trace amount of desired product was obtained when the reaction was performed at room temperature (Table 1, entry 12). It was worth noting, decreasing the stoichiometry of nitromethane (2 to 1.5 eq.) as well as sodium azide (3 to 2 eq.) affects reactivity and deliver the product in inferior yield (Table 1, entries 13, 14).

Intrigued by the exceptional reactivity of the newly synthesized catalyst, the effect of the ZnO catalyst amount was studied (Table 2, entries 1–7). From Table 2, it can be seen that excellent yield of the desired product was obtained within 2 h with 20 mg of catalyst (Table 2, entry 1). Decreasing the catalyst loading to 15 mg and 10 mg also afforded the desired NH-triazole in 2 h with magnificent yield (Table 2, entries 2, 3). With 5 mg of the catalyst, the reaction gave 98% yield in just 3 h (Table 2, entries 4, 7). However, a further decrease of catalyst loading resulted in decrease in yield

Scheme 2 Schematic diagram showing the formation of PEG capped ZnO nanoparticles under the reaction condition

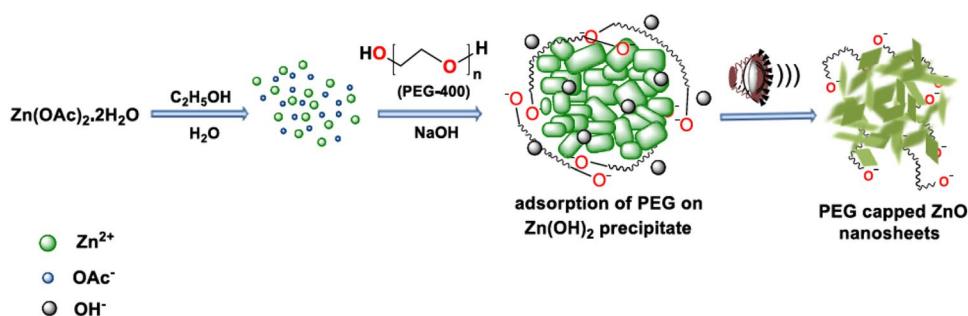
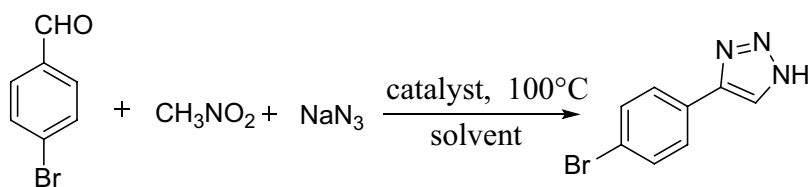


Table 1 Optimization of reaction conditions

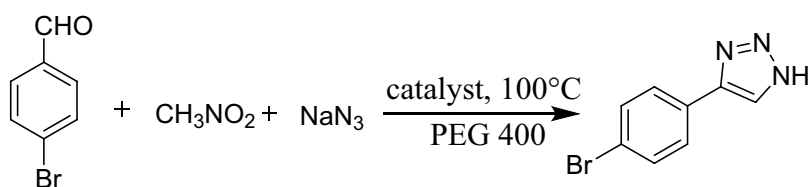
Entry	Solvent	Temperature	Time (h)	Yield ^a (%)
1	H ₂ O	100 °C	3	52
2	DCM	100 °C	3	75
3	DMF	100 °C	3	82
4	DMSO	100 °C	3	70
5	EG	100 °C	3	83
6	Toluene	100 °C	3	65
7	EG:H ₂ O	100 °C	3	79
8	DMF:H ₂ O	100 °C	3	75
9	DMSO:H ₂ O	100 °C	3	78
10	PEG-400	100 °C	3	98
11	PEG-400	80 °C	3	76
12	PEG-400	RT	24	Trace
13 ^b	PEG-400	100 °C	3	86
14 ^c	PEG-400	100 °C	3	72

Reaction conditions: 4-bromobenzaldehyde (1 mmol), nitromethane (2 mmol), NaN_3 (3 mmol), and catalyst (5 mg), solvent (3 mL), in air

^aIsolated yield

^bReaction was carried out with 1.5 eq. of nitromethane

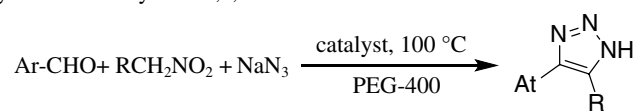
^cReaction was carried out with 2 eq. of NaN_3

Table 2 Optimization of catalyst loading in the synthesis of 4-aryl-NH-1,2,3-triazoles

Entry	Catalyst (mg)	Time (h)	Yield ^a (%)
1	20	2	98
2	15	2	98
3	10	2	98
4	5	3	98
5	2	4	70
6	-	3	25
7	5	2	84
		1	68

Reaction conditions: 4-bromobenzaldehyde (1 mmol), nitromethane (2 mmol), NaN_3 (3 mmol), catalyst, solvent (PEG-400) (3 mL), in air

^aIsolated yield

Table 3 Substrate scope for synthesis of 4-aryl-NH-1,2,3-triazoles

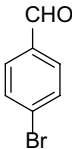
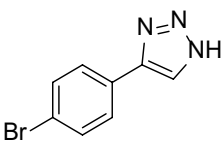
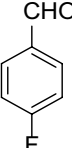
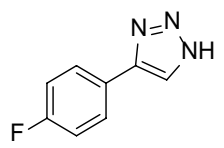
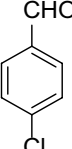
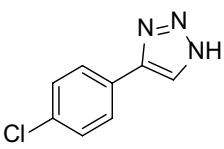
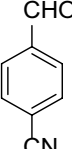
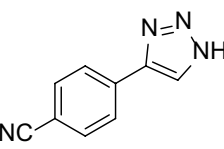
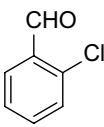
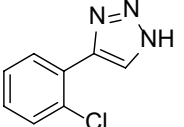
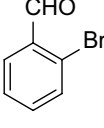
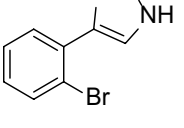
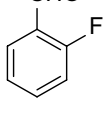
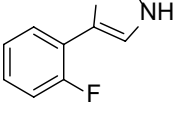
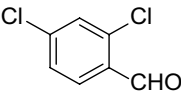
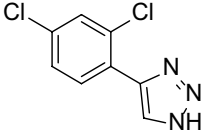
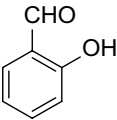
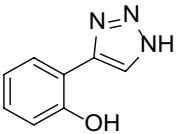
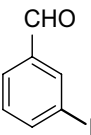
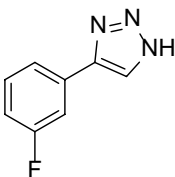
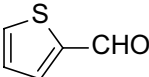
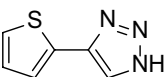
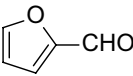
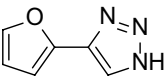
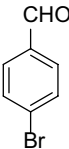
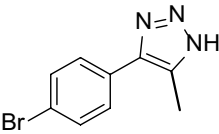
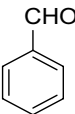
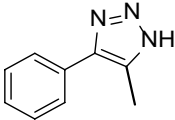
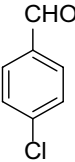
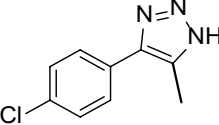
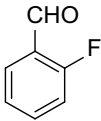
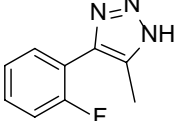
Entry	Aldehyde	Nitro alkane	Product	Time (h)	Yield ^b (%)
1		CH ₃ NO ₂		3	98
2		CH ₃ NO ₂		2	96
3		CH ₃ NO ₂		3	95
4		CH ₃ NO ₂		3	90
5		CH ₃ NO ₂		3	90
6		CH ₃ NO ₂		3	95
7		CH ₃ NO ₂		3	90

Table 3 (continued)

8		CH_3NO_2		2	98
9		CH_3NO_2		3	84
10		CH_3NO_2		3	86
11		CH_3NO_2		4	80
12		CH_3NO_2		4	77
13		$\text{CH}_3\text{CH}_2\text{NO}_2$		4	78
14		$\text{CH}_3\text{CH}_2\text{NO}_2$		4	73
15		$\text{CH}_3\text{CH}_2\text{NO}_2$		4	71
16		$\text{CH}_3\text{CH}_2\text{NO}_2$		3	86

Reaction conditions: aromatic aldehydes (1 mmol), nitroalkanes (2mmol), NaN_3 (3 mmol), catalyst (5 mg), PEG-400 (3 mL), 100 °C, in air^aIsolated yields

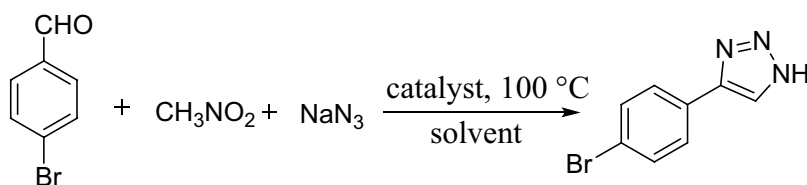
of the desired triazole along with increased reaction time (Table 2, entry 5). It is noteworthy to mention that when the reaction was carried out in the absence of the catalyst keeping other reaction parameters intact result obtained is quite unsatisfactory which enunciate the indispensability of the catalyst in order to obtain desired triazole in requisite time and yield. After exploring a wide spectrum of reaction conditions, 5 mg of ZnO-PEG catalyst in PEG-400 solvent was chosen as the optimised condition throughout this work.

Having established the optimized reaction conditions, a series of aldehydes were explored to investigate the substrate scope as summarised in Table 3 (entries 1–16). To our delight, the one-pot reaction condition adopted here afforded good yields of the desired NH-triazoles irrespective of whether functional group on the aldehyde is electron-withdrawing or electron-donating. In all cases, the ortho-, meta- and para-substituted aldehydes gave satisfactory yield of the corresponding products. Aromatic aldehydes bearing electron withdrawing functional groups such as halogen and cyanide displayed effective results with excellent yields of the NH-triazoles. Furthermore, salicylaldehyde and 2,4-dichlorobenzaldehyde also proceeded smoothly and afforded 84% and 98% yields respectively (Table 3, entries 8,9). Further, we examined the effect of heterocyclic moieties such as thiophen-2-aldehyde and furan-2-aldehyde for the synthesis of NH-triazoles. Heterocyclic compounds are of tremendous importance in the field of pharmaceutical sciences [53]. Hence, development of milder methodologies for the synthesis of these compounds is still a demanding task in the field of chemistry. Interestingly, these heterocyclic moieties are quite congenial with this transformation reaction (Table 3, entries 11, 12). In order to establish a broader

range of triazoles, we extended our study to another nitro compound that is nitroethane under standard reaction condition. Apparently, the reactions proceeded smoothly delivering the corresponding triazole products (3, entries 13–16). The spectral data of the purified triazole products are included in the supporting information (see Figure S2–S20).

An important factor that determines the efficiency of a heterogeneous catalytic system is its reusability. This factor serves to be beneficial both from commercial as well as green chemistry point of view [54]. To check the reusability of the catalyst as well as the solvent, consecutive one-pot multi-component reaction was performed by using 4-bromo benzaldehyde, nitromethane and sodium azide with PEG capped ZnO nanocatalyst and PEG-400 as solvent. We were gratified to observe that the PEG capped ZnO nanoparticles/PEG-400 system can be effectively re-used up to four catalytic cycles without significant loss of activity. After initial set of experiment, the reaction mixture containing products were extracted with diethyl ether (3×10 mL) leaving behind the catalyst dispersed in the PEG-400 solvent. For the next cycle of reaction, same substrates (4-bromo-benzaldehyde, nitromethane and sodium azide) were added with same stoichiometry without further addition of catalyst and solvent. The experimental results of consecutive four runs showed that the results were almost consistent in terms of yields and reaction rate up to 4th cycle, which confirmed the efficiency of the ZnO nano catalyst as well PEG-400 solvent system as recyclable catalytic system. The efficiency of reused catalyst is due to the unaltered morphology under the catalytic reaction condition after many cycles (See Figure S21 for TEM images of recovered catalyst) (Table 4).

Table 4 Recyclability of the catalytic system



Entry	Run	Time (h)	Yield ^a (%)
1	1st	3	98
2	2nd	3	98
3	3rd	3	97
4	4th	3	93

Reaction conditions: aromatic aldehydes (1 mmol), nitroalkanes (2 mmol), NaN₃ (3 mmol), catalyst (5 mg), PEG 400 (3 mL), 100 °C, in air

^aIsolated yield

4 Conclusion

Highly stable, pure hexagonal wurtzite structure of ZnO nanocrystals having plates/sheets type of architecture with sizes 15–25 nm have been prepared from $\text{Zn}(\text{OAc})_2 \cdot 2\text{H}_2\text{O}$ precursor in the presence of PEG-400 under ultrasonic irradiation. The as-synthesized nanoparticles were well characterized for structural purity and morphology study. The as-synthesized ZnO nanocrystals catalysed one-pot, three component reaction described here provides an efficient, facile and step-economic method for the synthesis of 4-aryl-NH-1,2,3-triazoles using aldehydes, nitroalkane and sodium azide in PEG 400 solvent. The reaction condition tolerated a wide array of electronically diverse substrates and also employed readily available cheap starting materials, thus providing a convenient approach for synthesis of these substituted NH-1,2,3-triazoles.

Acknowledgements D.S. is thankful to DST, New Delhi, India for a research grant [No. EMR/2016/002345]. S.A. is grateful to SERB, India for research fellowship. K.D. thanks SERB-DST, India (Grant EEQ/2018/000326) and UGC, India (Grant No.F.30-467/2019-BSR) for financial support. We thank Dibrugarh University for providing all the infrastructural facility, IIT-Delhi for FESEM and AIIMS, Delhi for HRTEM facility. The authors acknowledge the Department of Science and Technology for financial assistance under DST-FIST programme and UGC, New Delhi for Special Assistance Programme (UGC-SAP) to the Department of Chemistry, Dibrugarh University.

Compliance with Ethical Standards

Conflict of interest The authors declare no competing financial interest.

References

- Armstrong RW, Combs AP, Tempest PA, Brown SD, Keating TA (1996) Multiple-component condensation strategies for combinatorial library synthesis. *Acc Chem Res* 29:123–131
- Laurent A, Gerhardt CF (1838) Ueber einige Stickstoffverbindungen des Benzoyls. *Ann Chim Phys* 66:181–181
- Kakuchi R, Theato P (2013) Three-component reactions for post-polymerization modifications. *ACS Macro Lett* 2:419–422
- Pandey G, Singh RP, Garg A, Singh VK (2005) Synthesis of Mannich type products via a three-component coupling reaction. *Tetrahedron Lett* 46:2137–2140
- Garg A, Ali AA, Damarla K, Kumar A, Sarma D (2018) Aqueous bile salt accelerated cascade synthesis of 1,2,3-triazoles from arylboronic acids. *Tetrahedron Lett* 59:4031–4035
- Ali AA, Konwar M, Chetia M, Sarma D (2016) [Bmim] OH mediated Cu-catalyzed azide-alkyne cycloaddition reaction: a potential green route to 1,4-disubstituted 1,2,3-triazoles. *Tetrahedron Lett* 57:5661–5665
- Tornøe CW, Christensen C, Meldal M (2002) Peptidotriazoles on solid phase: [1,2,3]-triazoles by regioselective copper (I)-catalyzed 1, 3-dipolar cycloadditions of terminal alkynes to azides. *J Org Chem* 67:3057–3064
- Rostovtsev VV, Green LG, Fokin VV, Sharpless KB (2002) A stepwise Huisgen cycloaddition process: copper (I)-catalyzed regioselective “ligation” of azides and terminal alkynes. *Angew Chem Int Ed* 41:2596–2599
- Yang Y, Rasmussen BA, Shlaes DM (1999) Class A β -lactamases—enzyme-inhibitor interactions and resistance. *Pharmacol Ther* 83:141–151
- Dhumal ST, Deshmukh A, Kharat KR, Sathe BR, Chavan SS, Mane RA (2019) Copper fluorapatite assisted synthesis of new 1, 2, 3-triazoles bearing a benzothiazolyl moiety and their antibacterial and anticancer activities. *New J Chem* 43:7663–7673
- Ali AA, Gogoi D, Chaliha AK, Buragohain AK, Trivedi P, Saikia PJ, Gehlot PS, Kumar A, Chaturvedi V, Sarma D (2017) Synthesis and biological evaluation of novel 1, 2, 3-triazole derivatives as anti-tubercular agents. *Bioorg Med Chem Lett* 16:3698–3703
- Thirumurugan P, Matosiuk D, Jozwiak K (2013) Click chemistry for drug development and diverse chemical–biology applications. *Chem Rev* 113:4905–4979
- Liu YH, Zhang L, Xu XN, Li ZM, Zhang DW, Zhao X, Li ZT (2014) Intramolecular C–H...F hydrogen bonding-induced 1, 2, 3-triazole-based foldamers. *Org Chem Front* 1:494–500
- Lau YH, Rutledge PJ, Watkinson M, Todd MH (2011) Chemical sensors that incorporate click-derived triazoles. *Chem Soc Rev* 40:2848–2866
- Hanselmann R, Job GE, Johnson G, Lou RL, Martynow JG, Reeve MM (2010) Synthesis of an antibacterial compound containing a 1, 4-substituted 1 H-1, 2, 3-triazole: A scaleable alternative to the “click” reaction. *Org Process Res Dev* 14:152–158
- Chabre YM, Roy R (2008) Recent trends in glycodendrimer syntheses and applications. *Curr Top Med Chem* 8:1237–1285
- da Silva FDC, de Souza MCB, Frugulhetti II, Castro HC, Silmara LDO, de Souza TML, Rodrigues DQ, Souza AM, Abreu PA, Passamani F, Rodrigues CR (2009) Synthesis, HIV-RT inhibitory activity and SAR of 1-benzyl-1H-1, 2, 3-triazole derivatives of carbohydrates. *Eur J Med Chem* 44:373–383
- Bozorov K, Zhao J, Aisa HA (2019) 1,2,3-Triazole-containing hybrids as leads in medicinal chemistry: A recent overview. *Bioorg Med Chem* 27:3511–3531
- Rohrig UF, Awad OL, Grosdidier OA, Larrieu P, Stroobant V, Colau D, Cerundolo V, Simpson AJG, Vogel P, Van den Eynde BJ, Zoete V, Michielin O (2010) Rational design of indoleamine 2, 3-dioxygenase inhibitors. *J Med Chem* 53:1172–1189
- Panzarasa G (2018) Just Add Luminol to Turn the Spotlight on Radziszewski Amidation. *ACS Omega* 3(10):13179–13182
- Lanigan RM, Starkov P, Sheppard TD (2013) Direct synthesis of amides from carboxylic acids and amines using $\text{B}(\text{OCH}_2\text{CF}_3)_3$. *J Org Chem* 78(9):4512–4523
- Ghose AK, Viswanadhan VN, Wendoloski JJ (1999) *J Combin Chem* 1:55–68
- Carey JS, Laffan D, Thomson C, Williams MT (2006) *Org Biomol Chem* 4:2337–2347
- Suppo JS, de Figueiredo RM, Campagne JM (2003) Dipeptide Syntheses via Activated α -Aminoesters. *Org Synth* 92:296–308
- Chen Y, Wendt-Pienkowski E, Ju J, Lin S, Rajski SR, Shen B (2010) Characterization of FdmV as an amide synthetase for fredericamycin A biosynthesis in *Streptomyces griseus* ATCC 43944. *J Biol Chem* 285(50):38853–38860
- Valverde IE, Mindt TL (2013) 1, 2, 3-Triazoles as amide-bond surrogates in peptidomimetics. *CHIMIA International Journal for Chemistry* 67(4):262–266
- Weide T, Saldanha SA, Minond D, Spicer TP, Fotsing JR, Spaargaren M, Frère JM, Bebrone C, Sharpless KB, Hodder PS, Fokin VV (2010) NH-1, 2, 3-triazole inhibitors of the VIM-2 metallo- β -lactamase. *ACS Med Chem Lett* 1:150–154
- Röhrig UF, Majjigapu SR, Grosdidier A, Bron S, Stroobant V, Pilotte L, Colau D, Vogel P, Van den Eynde BJ, Zoete V, Michielin O (2012) Rational design of 4-aryl-1, 2, 3-triazoles for indoleamine 2, 3-dioxygenase 1 inhibition. *J Med Chem* 55:5270–5290

29. Tundo P, Anastas DS, Black J, Breen T, Collins S, Memoli J, Miyamoto M, Polyakoff M, Tumas W (2000) Synthetic pathways and processes in green chemistry. Introductory overview *Pure Appl Chem* 72:1207–1228
30. Boruah PR, Ali AA, Saikia B, Sarma D (2015) A novel green protocol for ligand free Suzuki-Miyaura cross-coupling reactions in WEB at room temperature. *Green Chem* 17:1442–1445
31. Hooshmand SE, Heidari B, Sedghi R, Varma RS (2019) Recent advances in the Suzuki-Miyaura cross-coupling reaction using efficient catalysts in eco-friendly media. *Green Chem* 21:381–405
32. Chen J, Spear SK, Huddleston JG, Rogers RD (2005) Polyethylene glycol and solutions of polyethylene glycol as green reaction media. *Green Chem* 7:64–82
33. Soh L, Eckelman MJ (2016) Green solvents in biomass processing. *ACS Sustain Chem Eng* 4:5821–5837
34. Borrell M, Costas M (2018) Greening oxidation catalysis: iron catalyzed alkene syn-dihydroxylation with aqueous hydrogen peroxide in green solvents. *ACS Sustain Chem Eng* 6:8410–8416
35. Feu KS, Alexander F, Silva S, de Moraes Junior MA, Corrêa AG, Paixão MW (2014) Polyethylene glycol (PEG) as a reusable solvent medium for an asymmetric organocatalytic Michael addition. Application to the synthesis of bioactive compounds. *Green Chem* 16:3169–3174
36. Pohlit H, Worm M, Langhanki J, Berger-Nicoletti E, Opatz T, Frey H (2017) Silver oxide mediated monotosylation of poly(ethylene glycol) (peg): heterobifunctional PEG via polymer desymmetrization. *Macromolecules* 50:9196–9206
37. Gu Y (2012) Multicomponent reactions in unconventional solvents: state of the art. *Green Chem* 14:2091–2128
38. Suresh D, Nethravathi PC, Rajanaika H, Nagabhushana H, Sharma SC (2015) Green synthesis of multifunctional zinc oxide (ZnO) nanoparticles using *Cassia fistula* plant extract and their photodegradative, antioxidant and antibacterial activities. *Mat Sci Semicon Proc* 31:446–454
39. Król A, Pomastowski P, Rafińska K, Railean-Plugaru V, Buszewski B (2017) Zinc oxide nanoparticles: Synthesis, antiseptic activity and toxicity mechanism. *Adv Colloid Interfac* 249:37–52
40. Strunk J, Kahler K, Xia X, Muhler M (2009) The surface chemistry of ZnO nanoparticles applied as heterogeneous catalysts in methanol synthesis. *Surf Sci* 603:1776–1783
41. Zhao W, Wei JS, Zhang P, Chen J, Kong JL, Sun LH, Xiong HM, Möhwald H (2017) Self-assembled ZnO nanoparticle capsules for carrying and delivering isotretinoin to cancer cells. *ACS Appl Mater Inter* 9:18474–18481
42. Jana A, Scheer E (2018) Study of optical and magnetic properties of graphene-wrapped ZnO nanoparticle hybrids. *Langmuir* 34:1497–1505
43. Sajjada M, Ullaha I, Khanb MI, Khanc J, Khana MY, Qureshid MT (2018) Structural and optical properties of pure and copper doped zinc oxide nanoparticles. *Results Phys* 9:1301–1309
44. Banerjee B (2017) Recent developments on nano-ZnO catalyzed synthesis of bioactive heterocycles. *J Nanostructure Chem* 7(4):389–413
45. Ravirajan P, Peiró AM, Nazeeruddin MK, Graetzel M, Bradley DDC, Durrant JR, Nelson, J (2006) Hybrid polymer/zinc oxide photovoltaic devices with vertically oriented ZnO nanorods and an amphiphilic molecular interface layer. *J Phys Chem B* 110:7635–7639
46. Errico V, Arrabito G, Fornetti E, Fuoco C, Testa S, Saggio G, Rufini S, Cannata S, Desideri A, Falconi C (2018) High-density ZnO nanowires as a reversible myogenic–differentiation switch. *ACS Appl Mater Inter* 10:14097–14107
47. Graces HF, Espinal AE, Suib SL (2012) Tunable shape microwave synthesis of zinc oxide nanospheres and their desulfurization performance compared with nanorods and platelet-like morphologies for the removal of hydrogen sulfide. *J Phys Chem C* 116:8465–8474
48. Lei Y, Luo N, Yan X, Zhao Y, Zhang G, Zhang Y (2012) A highly sensitive electrochemical biosensor based on zinc oxide nanotetrapods for L-lactic acid detection. *Nanoscale* 4:3438–3443
49. Zhang P, Xu F, Navrotsky A, Lee JS, Kim S, Liu J (2007) Surface enthalpies of nanophase ZnO with different morphologies. *J Chem Mater* 19:5687–5693
50. Sirelkhatim A, Mahmud S, Seeni A, Kaus NHM, Ann LC, Bakhor SKM, Hasan H, Mohamad D (2015) Review on zinc oxide nanoparticles: antibacterial activity and toxicity mechanism. *Nano-Micro Lett* 7:219–242
51. Fujimoto T, Terauchi S, Umehara H, Kojima I, Henderson W (2001) Sonochemical preparation of single-dispersion metal nanoparticles from metal salts. *Chem Mater* 13:1057–1060
52. Kushal DB, Fujita SI, Arai M, Pandit AB, Bhanage BM (2011) Ultrasound assisted additive free synthesis of nanocrystalline zinc oxide. *Ultrason Sonochem* 18:54–58
53. Kitamura Y, Sako S, Udzu T, Tsutsui A, Maegawa T, Monguchi Y, Sajiki H (2007) Ligand-free Pd/C-catalyzed Suzuki-Miyaura coupling reaction for the synthesis of heterobiaryl derivatives. *Chem Commun* 47:5069–5071
54. Boruah PR, Ali AA, Saikia B, Chetia M, Sarma D (2015) Pd(OAc)₂ in WERSA: a novel green catalytic system for Suzuki-Miyaura cross-coupling reactions at room temperature. *Chem Commun* 51:11489–11492

Publisher's Note Springer Nature remains neutral with regard to jurisdictional claims in published maps and institutional affiliations.